Proceedings of the 2nd International Conference on Mathematical Physics and Computational Simulation
DOI: 10.54254/2753-8818/39/20240620

A finite volume formulation for one-dimensional Stefan problems

Truman You

Basis Independent Silicon Valley, San Jose, 95126, the United States of America

feinanxu@gwu.edu

Abstract. This paper presents a numerical formulation that combines the finite-volume method with a time-dependent boundary-fitted coordinate system to tackle the moving boundary problems for the one-dimensional (1-D) heat equation. Following the formulation process, an algorithm was created with the help of the linear algebra package Eigen to generate the data for the numerical solution. Four benchmark cases of heat conduction were investigated by this approach and compared to the analytical solution: a fixed boundary case, the liquid phase of a melting process, the solid phase of a melting process, and an ablating process. The results demonstrate the capability of the presented numerical formulation in efficiently solving the general 1-D heat problems, especially the one-phase Stefan problems, as well as the consistency of the numerical and analytical solutions. Future works can strive to extend the formulations to Stefan problems of two phases or higher dimensions. The work can then be extended to real-life applications, such as the spacecraft re-entry ablation process, and the process of iceberg melting, demonstrating its critical value in solving practical problems.

Keywords: Finite volume method, Free boundary, Ablation heat transfer

1. Introduction

Many heat conduction problems encountered in science, engineering, and industry are associated with material solidification or melting processes, such as the metal and glass molding process, or space vehicle nose cone ablation during atmospheric re-entry. They are categorized as moving boundary problems due to the change of phase under certain physical situations. Since the moving boundary location is unknown in the heat equation which interacts with the temperature function in time, this type of heat equation is inherently non-linear. A considerable number of analytical and numerical works have been devoted to the Stefan problems. Ewing et al. [1] utilized a front-tracking method that is based on the variable control-volume grid to solve 1-D ablation heat transfer problems. Javierre et al. [2] conducted a numerical study on two-phase Stefan problems using three numerical methods: the moving grid, the level set, and the phase field methods. Finite mediums were developed by Kar and Mazumder [3]. A comparative study of BIM and VSG techniques in the solution to a one-phase Stefan problem was performed by Kutluay et al. [4]. This study concluded that both the moving grid and the level set methods show comparable accuracy and are suitable methods for modeling phase-change problems. Several numerical researches were conducted on ablation-type Stefan problems. Mitchell and Vynnycky [5] employed the Boundary Immobilization Method (BIM) in tandem with finite difference schemes to treat the start-up of the initially zero-thickness condition. Mitchell and Vynnycky [6] applied the

DOI: 10.54254/2753-8818/39/20240620

boundary immobilization method coupled with a Keller box finite-difference scheme to analyze the solution to 1-D ablation-type problems. In their approach, a pre-ablation analytical solution was applied as the initial condition at the onset of the ablation. Savoric and Caldwell [7] applied the Variable Space Grid (VSG) method in the finite difference scheme for front-tracking of the moving boundary. The problem of ice melting was first treated by Stefan [8], and therefore such problems are widely referred to as the Stefan problems. The analytical solution for semi-infinite mediums were developed by Tao [9].

In this study, a boundary-fitted grid explicitly tracks the moving front of the medium and is combined with the implicit finite-volume scheme to solve the one-phase one-dimensional Stefan problems. For ablation types of problems, the phase transition from the fixed boundary to the free boundary can be automatically identified and addressed in the numerical method.

2. Problem statement

2.1. Mathematical formulation

A general form of the 1-D heat equation in the Cartesian coordinates is given as

$$\frac{\partial T}{\partial t} = \alpha \frac{\partial^2 T}{\partial x^2} + F(x,t), \quad x_0 < x < x_1, \ t_0 < t < t_1 \tag{1}$$

in which $\alpha > 0$ denotes the thermal diffusivity of the material, and $F(x,t)$ represents a forcing function. For the homogeneous equation, $F(x,t)$ is set to zero.

For a fixed boundary problem, the initial and boundary conditions are defined in a general form as (2)-(4), respectively.

$$T(x,t_0) = T_0(x) \tag{2}$$

$$\beta_0 T(x_0,t) + \gamma_0 \frac{\partial T}{\partial x}|_{x=x_0} = f_0(t), \tag{3}$$

$$\beta_1 T(x_1,t) + \gamma_1 \frac{\partial T}{\partial x}|_{x=x_1} = f_1(t). \tag{4}$$

In boundary conditions (3) and (4), $\beta_0, \beta_1, \gamma_0, \gamma_1$ are prescribed constants such that $|\beta_0| + |\gamma_0| > 0, |\beta_1| + |\gamma_1| > 0$. $f_0(t), f_1(t)$ are prescribed functions of time. In (3), a Neumann type condition is recovered if $\beta_0 = 0, \gamma_0 = 1$, whereas a Dirichlet type condition is recovered if $\beta_0 = 1, \gamma_0 = 0$. It is likewise in (4).

For a moving boundary problem, due to phase change (such as melting of the solid phase) at a boundary, either point at x_0 or x_1 becomes a free boundary at a time $t > t_0$. The free boundary can be tracked by the introduction of a location function $s(t)$. The initial location of the free boundary $s(t_0)$ needs to be specified as in (5). To represent a constant temperature during the phase change process, a Dirichlet condition with a time-independent constant f is imposed at the free boundary. Therefore, the corresponding condition (3) or (4) at the location $s(t)$ would be replaced by the condition (6) below. Furthermore, the Stefan condition (7), which essentially defines the energy balance at the free boundary, is required to close the system of equations.

$$s(t_0) = s_0, \tag{5}$$

$$\beta T(s,t) = f, \tag{6}$$

$$\lambda \frac{ds}{dt} = -\frac{\partial T}{\partial x}(s(t),t), \tag{7}$$

in which s_0, f, λ are constants, and $\lambda > 0$.

In summary, a fixed boundary problem is defined by Eqs. (1)-(4), and a moving boundary problem is defined by Eqs. (1)-(7).

DOI: 10.54254/2753-8818/39/20240620

2.2. Numerical formulation

The numerical solution to the heat equation with a moving boundary requires the discretization of the equation to be based on a time-dependent boundary-fitted grid, which can be achieved by the transformation from the physical coordinates (x,t) into the computational coordinates (ξ,τ) defined as follows:

$$\xi = \xi(x,t), \quad \xi:\ i = 0,1,\dots,i_{max}, \tag{8}$$

$$\tau = \tau(t), \quad \tau:\ j = 0,1,\dots,j_{max}. \tag{9}$$

$$So, \quad x = x(i,j), \quad t = t(j). \tag{10}$$

Introducing the Jacobian J to represent the transformation of the metric [10], the relationship between two coordinate systems is defined as

$$J = \frac{\partial(\xi,\tau)}{\partial(x,t)} = |\xi_x\ \xi_t\ \tau_x\ \tau_t\ |, \xi_x = \frac{1}{x_\xi}, \xi_t = \frac{-x_\tau}{x_\xi}, \tau_x = 0, \tau_t = 1; \tag{11}$$

in which $\Delta\xi = 1$, $x_\xi(i,j) = x(i+1,j) - x(i,j)$, and $\Delta\tau = \Delta t(j) = t(j+1) - t(j)$, $x_\tau(i,j) = \frac{x(i,j+1)-x(i,j)}{t(j+1)-t(j)}$.Then, $x_{\xi\xi}(i,j) = x_\xi(i,j) - x_\xi(i-1,j)$.

After the coordinate transformation, the governing equation (1) based on the computational coordinates (ξ,τ) can be written as

$$\frac{\partial T}{\partial \tau} - \frac{x_\tau}{x_\xi}\frac{\partial T}{\partial \xi} = \frac{\alpha}{(x_\xi)^2}\frac{\partial^2 T}{\partial \xi^2} - \alpha\frac{x_{\xi\xi}}{(x_\xi)^3}\frac{\partial T}{\partial \xi} + F(\xi,\tau). \tag{12}$$

It should be noted that the coordinates (ξ,τ) should be generated every time step to conform to the moving boundary. Hence, the Jacobian J is updated in time to yield time-accurate metric coefficients in Equation (12). The discretization of Equation (12) uses the central difference scheme in space and a fully implicit scheme in time. So for the ith cell and the jth time step $(x(i,j) < x < x(i+1,j), t(j))$, the domain functions (T,F) and coefficients (A,B,C,D,E,G) are evaluated at the cell center and denoted like $T_{i+1/2,j}$ for instance. Therefore the discretized equation is given as:

$$C_{i+1/2,j} * T_{i-1/2,j+1} + A_{i+1/2,j} * T_{i+1/2,j+1} + B_{i+1/2,j} * T_{i+3/2,j+1}$$
$$= E_{i+1/2,j} * T_{i-1/2,j} + D_{i+1/2,j} * T_{i+1/2,j} + G_{i+1/2,j} * T_{i+3/2,j} + F_{i+1/2,j}, \tag{13}$$

where

$$A_{i+1/2,j} = \frac{1}{\Delta\tau} + \frac{2\alpha}{(x_\xi)^2}, \tag{14}$$

$$B_{i+1/2,j} = \frac{-x_\tau}{2x_\xi} - \frac{\alpha}{(x_\xi)^2} + \frac{\alpha x_{\xi\xi}}{2(x_\xi)^3}, \tag{15}$$

$$C_{i+1/2,j} = \frac{x_\tau}{2x_\xi} - \frac{\alpha}{(x_\xi)^2} - \frac{\alpha x_{\xi\xi}}{2(x_\xi)^3}, \tag{16}$$

$$D_{i+1/2,j} = \frac{1}{\Delta\tau}, \tag{17}$$

$$E_{i+1/2,j} = 0, \tag{18}$$

$$G_{i+1/2,j} = 0. \tag{19}$$

The boundary conditions (3)(4) in the computational domain (ξ,τ) are rewritten as:

$$\beta_0 T_{i,j}|_{i=0} + \frac{\gamma_0}{x_\xi}\frac{\partial T_{i,j}}{\partial \xi}|_{i=0} = f_0(t(j)), \tag{20}$$

$$\beta_1 T_{i,j}|_{i=i_{max}} + \frac{\gamma_1}{x_\xi}\frac{\partial T_{i,j}}{\partial x}|_{i=i_{max}} = f_1(t(j)). \tag{21}$$

DOI: 10.54254/2753-8818/39/20240620

Hence the system of Equations (13)-(21) are put together to solve for the cell center value $T_{i+1/2,j+1}$, $(0 \le i < i_{max})$, in the matrix form as:

$$\begin{bmatrix} (\frac{\beta_0}{2} - \frac{\gamma_0}{x_\xi}) & (\frac{\beta_0}{2} + \frac{\gamma_0}{x_\xi}) & 0 & \cdots & 0 \\ C_{1/2,j} & A_{1/2,j} & B_{1/2,j} & \ddots & \vdots \\ 0 & \ddots & \ddots & \ddots & 0 \\ \vdots & \ddots & C_{i_{max}-\frac{1}{2},j} & A_{i_{max}-\frac{1}{2},j} & B_{i_{max}-\frac{1}{2},j} \\ 0 & \cdots & 0 & (\frac{\beta_1}{2} - \frac{\gamma_1}{x_\xi}) & (\frac{\beta_1}{2} + \frac{\gamma_1}{x_\xi}) \end{bmatrix} \begin{bmatrix} T_{-1/2,j+1} \\ T_{1/2,j+1} \\ \vdots \\ T_{i_{max}-\frac{1}{2},j+1} \\ T_{i_{max}+\frac{1}{2},j+1} \end{bmatrix}$$

$$= \begin{bmatrix} 0 & 0 & 0 & \cdots & 0 \\ G_{1/2,j} & D_{1/2,j} & E_{1/2,j} & \ddots & \vdots \\ 0 & \ddots & \ddots & \ddots & 0 \\ \vdots & \ddots & G_{i_{max}-\frac{1}{2},j} & D_{i_{max}-\frac{1}{2},j} & E_{i_{max}-\frac{1}{2},j} \\ 0 & \cdots & 0 & 0 & 0 \end{bmatrix} \begin{bmatrix} T_{-1/2,j} \\ T_{1/2,j} \\ \vdots \\ T_{i_{max}-\frac{1}{2},j} \\ T_{i_{max}+\frac{1}{2},j} \end{bmatrix} + \begin{bmatrix} f_0(t(j+1)) \\ F_{1/2,j} \\ \vdots \\ F_{i_{max}-\frac{1}{2},j} \\ f_1(t(j+1)) \end{bmatrix} \quad (22)$$

It should be noted that the first and the last rows of Equation (22) address the boundary conditions (20) and (21), in which $T_{-1/2,j+1}, T_{i_{max}+\frac{1}{2},j+1}$ correspond to the mirror cells of their neighboring cells with respect to the endpoints at $i = 0$ and $i = i_{max}$. For the moving boundary case, either γ_0 or γ_1 is set to 0 so that Equation (6) can be recovered in the matrix form (22).

The numerical formulation (22) is applied to solve for the temperature distribution $T(x,t)$ in the fixed and the moving boundary problems. For the moving boundary problems, in addition to $T(x,t)$, Equation (23) which is the transformed form of (7) is utilized to update the free boundary location $s(t)$ at the end of the jth times step $t(j)$. Hence, the overall numerical scheme is semi-implicit in time: implicit for updating the temperature distribution $T(x,t)$ and explicit for updating the free boundary location $s(t)$.

$$\lambda \frac{ds}{dt}|_{t=t(j)} = -\frac{\frac{\partial T}{\partial \xi}|_{i,j}}{x_\xi(i,j)}, \ for \ s(t) \ at \ i = 0 \ or \ i = i_{max} \quad (23)$$

2.3. Solution algorithm

The numerical simulation of the 1-D heat equation with a moving boundary consists of solving the governing equation, updating the boundary location, and generating the boundary-fitted grid in a time-accurate manner. An algorithm designed to solve the dynamic system in an iterative procedure is summarized as follows:

(1) At initial time $j = 0$, apply s_0 to the initial moving boundary location (x_0 or x_1). Generate an initial grid in ξ-coordinate ($0 \le i \le i_{max}$) bounded by two specified boundary positions (x_0, x_1) in the spatial domain.

(2) Update domain functions of T,F and the coefficients A, B, C, D, E, G in the governing Equation (22) at time $t(j)$.

(3) Apply the Stefan condition (23) to update the moving boundary position s at time $t(j+1)$. Regenerate the grid in ξ-coordinate ($0 \le i \le i_{max}$) based on updated boundary locations at time $t(j+1)$.

(4) Solve Equation (22) for T at $t(j+1)$ with the time interval of $\Delta t(j)$ by employing the matrix solver of the linear algebra library *Eigen*.

(5) Update $j = j + 1$ for the next time step, return to Item 2 and go through the solution procedures again. The iterative process continues until either the phase-vanishing time or a prescribed final time t_1 is met at $j = j_{max}$.

DOI: 10.54254/2753-8818/39/20240620

3. Results and discussion

3.1. Case 1: a fixed boundary problem

In general, a 1-D heat equation with fixed boundary conditions can be dealt with by the method of separation of variables for analytical solutions. Following Greenberg [11], the fixed-boundary heat problem is considered for a comparison of its analytical and computational results. In this case, both Neumann and Dirichlet boundary conditions are imposed at the endpoints.

$$\alpha T_{xx} = T_t - e^{-t}cos(\frac{\pi x}{2L}), \quad (0 \le x \le L,\ 0 \le t < t_1) \tag{24}$$

$$T_x(0,t) = T(L,t) = 0, \quad T(x,0) = 0. \tag{25}$$

The exact analytical solution to this problem was obtained as

$$T(x,t) = \frac{e^{-t} - e^{-(\frac{\pi}{2L})^2 \alpha t}}{(\frac{\pi}{2L})^2 \alpha - 1} cos(\frac{\pi x}{2L}) \tag{26}$$

This problem was then modeled by the method described in the previous section. The computational domain is composed of uniformly spaced cells in length (Δx) and in time (Δt), respectively. To make a straight comparison between numerical and analytical results, the parameters $\alpha = 2.0,\ L = 1.0,\ t_1 = 5.0$ were selected for presented results. Different levels of refinement on the computational grid were applied to check the convergence of numerical results. Table 1 presents a comparison of analytical and numerical results at $t = 0.5$. It shows a convergence of numerical results to the exact solution as the grid refinement increases. It was also observed that the numerical accuracy is more sensitive to the time refinement than to the spatial refinement in this case. Figure 1(a) displays an overview of the numerical solution $T(x,t)$ for the grid with $\Delta x = 0.05,\ \Delta t = 0.016$. The evolution of $T(x,t)$ displays a decoupled behavior in space and time, which is also implied in the analytical solution. The distribution of $T(x,t)$ at different time instants are compared well to their analytical counterparts, as shown in Figure 1(b).

Table 1. The impact of different grid refinements on numerical accuracy

x	$i_{max} = 20, j_{max} = 100$	$i_{max} = 20, j_{max} = 300$	$i_{max} = 100, j_{max} = 300$	$i_{max} = 20, j_{max} = 1000$	Analytical
0.000	0.133418	0.132845	0.132889	0.132639	0.132593
0.025	0.133418	0.132845	0.13279	0.132639	0.13249
0.075	0.132595	0.132026	0.131972	0.131821	0.131674
0.125	0.130955	0.130393	0.130339	0.130191	0.130045
0.175	0.128508	0.127956	0.127903	0.127757	0.127614
0.225	0.125268	0.124731	0.124679	0.124537	0.124397
0.275	0.121256	0.120736	0.120686	0.120548	0.120413
0.325	0.116496	0.115997	0.115948	0.115816	0.115687
0.375	0.111018	0.110542	0.110496	0.11037	0.110247
0.425	0.104856	0.104406	0.104363	0.104244	0.104127
0.475	0.098047	0.097627	0.097586	0.097475	0.097366
0.525	0.090634	0.090245	0.090208	0.090105	0.090004
0.575	0.082662	0.082307	0.082273	0.082179	0.082087
0.625	0.07418	0.073862	0.073831	0.073747	0.073665
0.675	0.065241	0.064961	0.064934	0.06486	0.064788
0.725	0.0559	0.05566	0.055637	0.055573	0.055511
0.775	0.046214	0.046016	0.045996	0.045944	0.045893
0.825	0.036243	0.036087	0.036072	0.036031	0.035991
0.875	0.026049	0.025937	0.025926	0.025897	0.025868

DOI: 10.54254/2753-8818/39/20240620

Table 1. (continued).

0.925	0.015694	0.015626	0.01562	0.015602	0.015585
0.975	0.005242	0.00522	0.005217	0.005211	0.005206
1.000	0	0	0	0	0

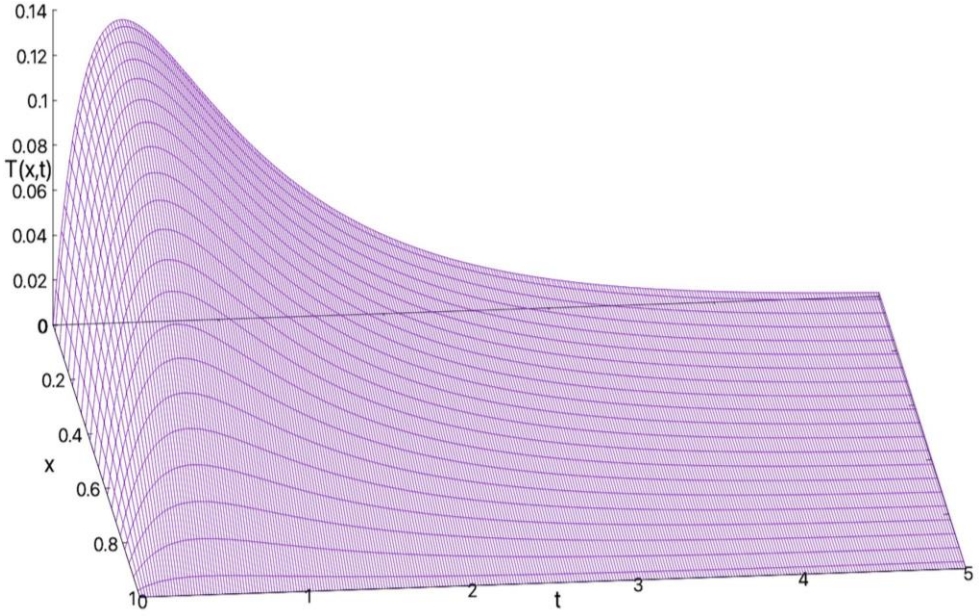

(a)

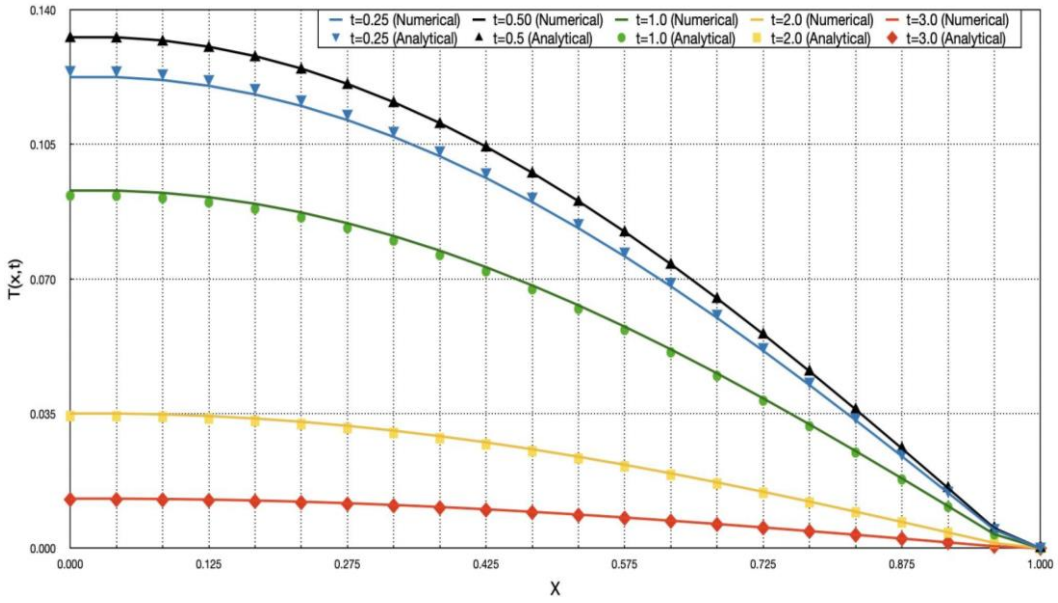

(b)

Figure 1. T(x,t) evolution in time and space: Δt = 0.016. (a) Overview of T(x,t) in time and space; (b)T(x,t): analytical vs numerical.

3.2. Case 2: a one-phase stefan problem with zero-thickness start-up

In this case, a single-phase Stefan problem was studied, assuming an initial thickness of zero in the region. Physically this situation is similar to the liquid phase evolution during the melting process. The governing equation for temperature $T(x,t)$ is given as:

DOI: 10.54254/2753-8818/39/20240620

$$\frac{\partial T}{\partial t} = \frac{\partial^2 T}{\partial x^2}, \quad 0 \le x \le s(t), \ t \ge 0, \tag{27}$$

subject to the boundary conditions:

$$T(x = 0, t) = T_0(t), \quad t \ge 0, \tag{28}$$

$$T(x = s(t), t) = 0, \quad t \ge 0, \tag{29}$$

and the Stefan condition of the free boundary $s(t)$:

$$\frac{ds}{dt} = -\frac{\partial T}{\partial x}, \quad x = s(t), \ t \ge 0, \tag{30}$$

and the initial conditions:

$$T(x, t = 0) = 0, \tag{31}$$

$$s(t = 0) = 0 \ . \tag{32}$$

If $T_0(t) = e^t - 1$ is specified, the analytical solution can be easily determined as:

$$T(x, t) = e^{(t-x)} - 1, \tag{33}$$

$$s(t) = t \ . \tag{34}$$

A common difficulty encountered by "front-tracking" numerical methods in dealing with this kind of "initial zero-thickness" Stefan problem was how the computation could be started at $t = 0$ when the spatial domain is still just a point (32). In the present work, the numerical treatment of this initial zero point is rather straightforward: Given the initial state $T = 0$ at $t = 0$ & $s = 0$, kickoff with a small $\Delta t > 0$ as the first-time step and assume the corresponding spatial movement of $s(\Delta t) = \Delta s = \Delta t$. Then, the computational domain can be constructed for the region $0 \le x \le s(\Delta t)$, and the numerical solution for $T(x, t)$ can be determined by Equation (22) for $t = \Delta t$. Next, Equation (23) is utilized to update $s(t)$ again. The solution for subsequent temporal and spatial steps will be obtained thereafter.

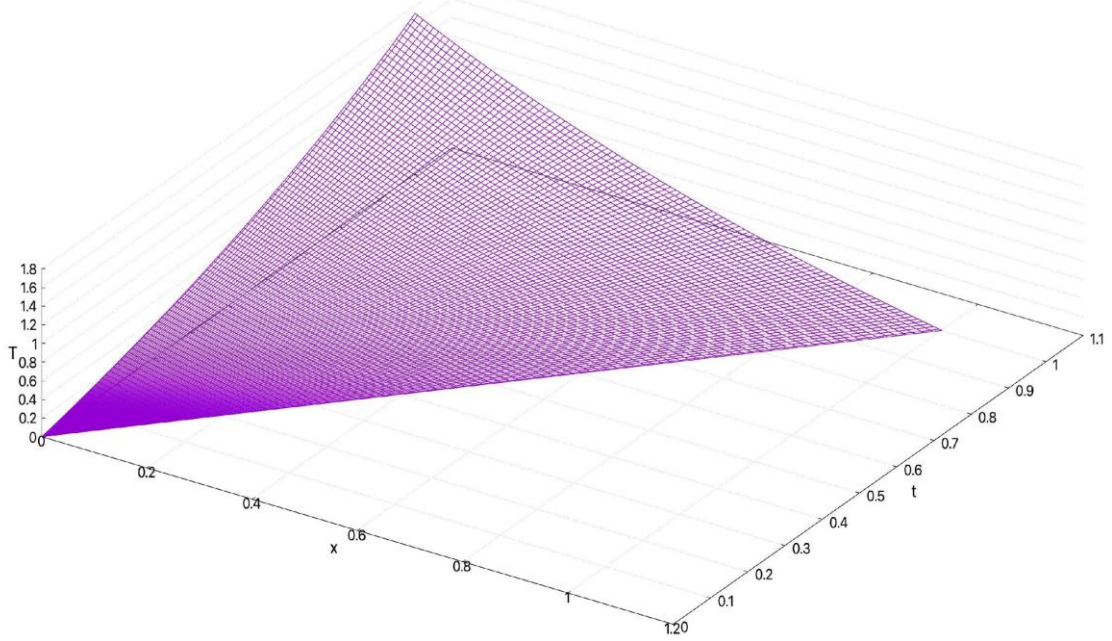

Figure 2. Overview of temperature and the moving boundary evolution in space and time (imax = 100, jmax = 100)

DOI: 10.54254/2753-8818/39/20240620

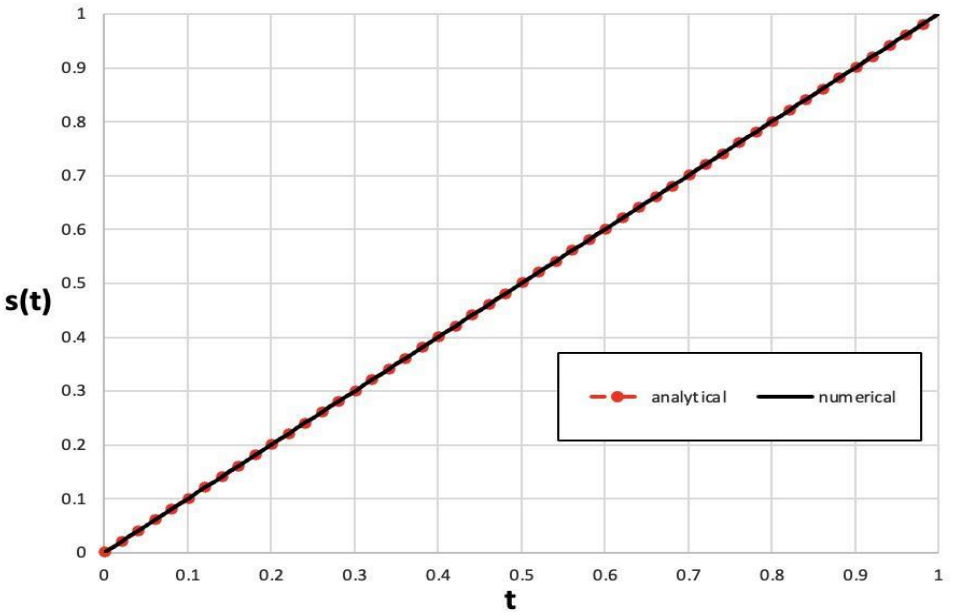

(a)

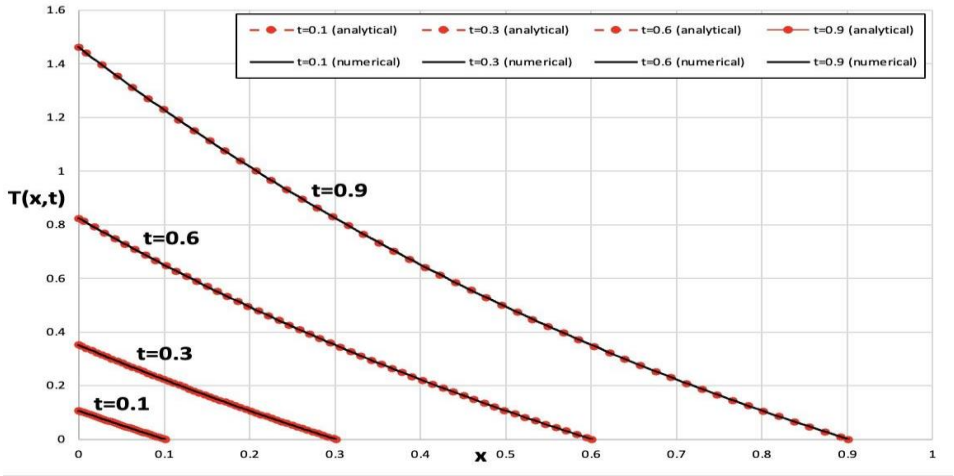

(b)

Figure 3. The temperature profile $T(x,t)$ and the moving boundary $s(t)$: analytical vs numerical, Δt = 0.01. (a) s(t) vs t; (b) T(x,t) vs t

The computational domain consists of equally spaced cells in x and t with Δx changing in time, and a constant $\Delta t = 0.01$ ($j_{max} = 100$) throughout the computation. Figure 2 presents an overview of $T(x,t)$ and $s(t)$ development in space and time. Figure 3 presents the comparison of analytical and numerical solutions for $s(t)$ and $T(x,t)$. As Figures 2 and 3 show, a good agreement was achieved between the two solutions.

3.3. Case 3: a one-phase Stefan problem with finite phase-varnishing time

In this case, a one-phase Stefan problem with finite phase-varnishing time is studied. Physically this situation is similar to the solid phase evolution in a melting process. Also, the problem is studied in a parametric form to obtain a general solution. The solid phase temperature distribution $T(x,t)$ and the free boundary location $s(t)$ are defined by a system of equations in a dimensionless form as shown below.

DOI: 10.54254/2753-8818/39/20240620

$$\frac{\partial T}{\partial t} = \alpha \frac{\partial^2 T}{\partial x^2}, \quad 0 \le x \le s(t), \ t \ge 0, \tag{35}$$

$$T(x = 0, t) = T_0(t), \quad t \ge 0, \tag{36}$$

$$T(x = s(t), t) = 0, \quad t \ge 0, \tag{37}$$

$$\frac{ds}{dt} = -\beta \frac{\partial T}{\partial x}(s(t), t), \quad t > 0, \tag{38}$$

$$s(t = 0) = s_0, \tag{39}$$

in which α, β, s_0 in (35)-(39) are prescribed positive constants. The boundary condition $T_0(t)$, however, could not be an arbitrary function if an analytical solution is sought. In order to make the analytical solution available, certain form has to be assumed for $T_0(t)$ as discussed later in the section.

By introducing a similarity variable $\xi = \frac{s_0 - x}{\sqrt{(t)}}$ and then assuming $T(x, t) = F(\xi(x, t))$, Equation (35) can be converted into a 2^{nd}-order ODE in terms of $F(\xi)$ as

$$\frac{d^2 F}{d\xi^2} + \frac{\xi}{2\alpha} \frac{dF}{d\xi} = 0. \tag{40}$$

A general solution to the problem can be obtained as

$$F = C_1 erf(\frac{\xi}{2\sqrt{\alpha}}) + C_2. \tag{41}$$

By substituting $T(x, t)$ into $F(\xi)$

$$T(x, t) = C_1 erf(\frac{s_0 - x}{2\sqrt{\alpha t}}) + C_2, \tag{42}$$

in which $erf(z) = \frac{2}{\sqrt{\pi}} \int_0^z \quad e^{-t^2} dt$ denotes an error function. The two constant coefficients C_1 and C_2 must satisfy the two boundary conditions (36),(37). So

$$\lambda = \frac{s_0 - s(t)}{2\sqrt{\alpha t}}, \tag{43}$$

$$C_1 = \frac{T_0(t)}{erf(\frac{s_0}{2\sqrt{\alpha t}}) - erf(\lambda)}, \tag{44}$$

$$C_2 = -C_1 erf(\lambda). \tag{45}$$

in which a new parameter λ is introduced for convenience. From (43)-(45) it is determined that $\lambda > 0$ is a constant. Then by utilizing (42)-(44) to substitute λ and C_1 into the Stefan condition (38), the following transcendental relationship between λ and C_1 is obtained

$$-\lambda e^{\lambda^2} = \frac{\beta C_1}{\alpha\sqrt{\pi}} \ . \tag{46}$$

As per (44), the boundary condition for $T_0(t)$ can be defined as the function of λ in the form of

$$T_0(t) = \frac{-\lambda e^{\lambda^2} \alpha\sqrt{\pi}}{\beta} [erf(\frac{s_0}{2\sqrt{\alpha t}}) - erf(\lambda)] \ . \tag{47}$$

Hence, if the four parameters $\alpha, \beta, s_0, \lambda$ are specified as positive constants, and $T_0(t)$ is defined in the form of (47), then the analytical solution to the problem can be determined for $T(x, t)$ and $s(t)$ as shown below.

$$T(x, t) = \frac{-\lambda e^{\lambda^2} \alpha\sqrt{\pi}}{\beta} [erf(\frac{s_0 - x}{2\sqrt{\alpha t}}) - erf(\lambda)], \tag{48}$$

$$s(t) = s_0 - 2\lambda\sqrt{\alpha t}. \tag{49}$$

From (46), the initial condition for $T(x, t = 0)$ is determined as

DOI: 10.54254/2753-8818/39/20240620

$$T(x,0) = T_0(0), \quad 0 \le x < s_0. \tag{50}$$

A numerical study was conducted for parameters $\alpha = \beta = s_0 = \lambda = 1$. As per (49), the phase-vanishing time is determined as $t_1 = 0.25$. For this case, the numerical setting consists of an equally spaced grid with $i_{max} = 200$ and a constant Δt in the computation. Then, the numerical results are compared to the exact solutions (48), (49) in the above analysis. Figure 4 presents the temperature profile $T(x,t)$ and the free boundary location $s(t)$ for the exact solution. As the time limit of 0.25 is approached, $s(t)$ moves towards the phase varnish point at $x = 0$, while $T(0,t)$ rises towards $T(s,t) = 0$. Figure 5(a) shows the numerically computed trajectory of the free boundary $s(t)$ for different Δt options. As Δt decreases, the computed trajectory converges to the analytical trajectory. However, small deviation is still observed near the end of the transient ($t > 0.2$) for $\Delta t = 2.5e-5$. Figure 5(b) presents a comparison of analytical and numerical temperature distributions along the length in the x-axis at different time instants. As the figure shows, the numerical result generally agrees well with the analytical data while it starts to display noticeable deviation between the two when $t = 0.2$. This deviation is attributed to numerical singularity which arises when the phase-varnishing point ($s(t) = 0$ is approached.

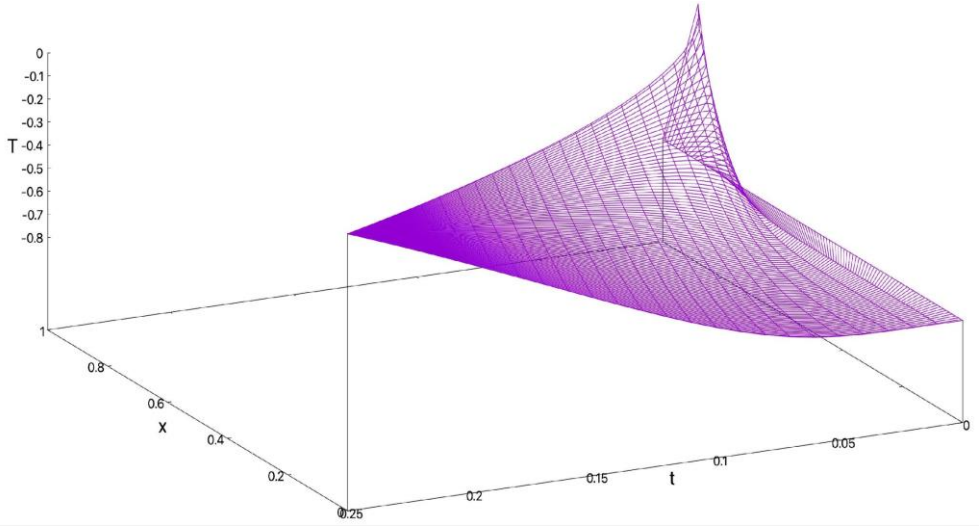

Figure 4. Temperature and the moving boundary of the exact solution

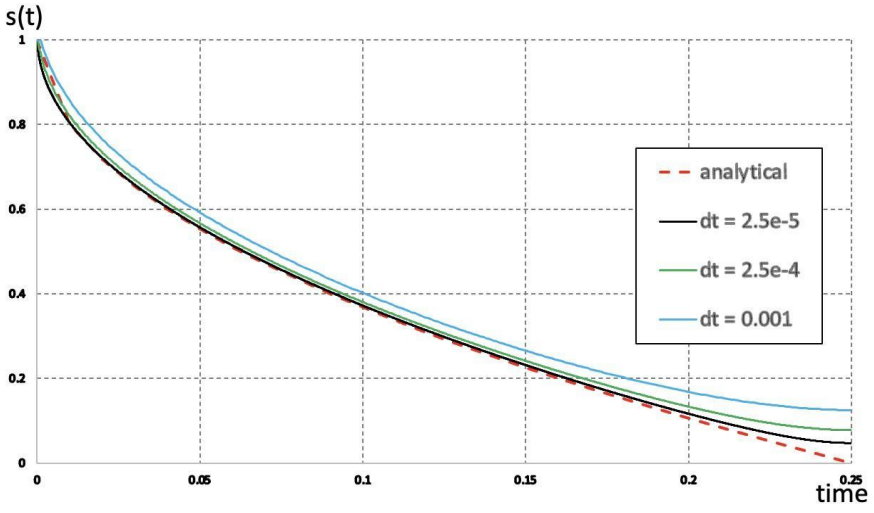

(a)

DOI: 10.54254/2753-8818/39/20240620

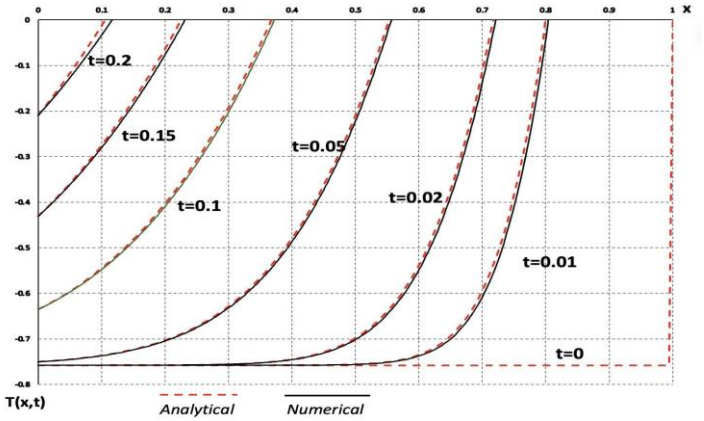

(b)

Figure 5. The comparison of solutions for s and T: analytical vs numerical. (a) The model predicted trajectories of the moving boundary s(t) for different time refinement levels; (b) Comparison of the numerical (Δt=2.5e−5, imax=200) and the exact solutions at various time instants.

3.4. Case 4: an ablation-type Stefan problem

An ablation-type one-phase one-dimensional Stefan problem is considered in the following dimensionless form:

$$\frac{\partial T}{\partial t} = \alpha \frac{\partial^2 T}{\partial x^2}, \quad 0 \le x \le L, \ t \ge 0, \tag{51}$$

subject to the initial condition:

$$T(x,0) = T_0, \quad 0 \le x \le L, \tag{52}$$

and the BCs before the onset of ablation at t_0:

$$T(L,t) = T_0, \quad 0 \le t \le t_0, \tag{53}$$

$$\frac{\partial T}{\partial x}(0,t) = -\beta, \quad 0 \le t \le t_0, \tag{54}$$

and the BCs after the onset of ablation at t_0:

$$T(L,t) = T_0, \quad t > t_0, \tag{55}$$

$$T(s(t),t) = T_m, \quad t > t_0, \tag{56}$$

$$s(t_0) = 0, \tag{57}$$

$$\lambda \frac{ds}{dt} = -(\beta_m + \frac{\partial T}{\partial x}(s(t),t), \quad t > t_0. \tag{58}$$

The parameters L, α, λ are positive constants corresponding to the spatial domain, thermal diffusivity and the reciprocal of Stefan number, respectively. β, β_m are positive constants associated with the heat flux imposed at the free boundary before and after the ablation, respectively. T_0, T_m correspond to the boundary temperatures. For convenience, the ablation onset time is set at $t_0 > 0$.

The system described by (51)-(58) represents a two-stage heat-up process: a normal heat-up process with no phase-change before time t_0, and the ablating heat transfer process after time t_0 when the Stefan condition (58) kicks in. For $0 \le t \le t_0$, the above equations (51)-(54) represent a classical 1-D heat equation with fixed boundary conditions. The analytical solution can be obtained by the method of Separation of Variables:

$$T(x,t) = \beta(L-x) + T_0 - \sum_{n=1,3,5,\ldots}^{\infty} [\frac{8\beta L}{(n\pi)^2} cos(\frac{n\pi x}{2L}) e^{-(\frac{n\pi\alpha}{2L})^2 t}]. \tag{59}$$

DOI: 10.54254/2753-8818/39/20240620

It should be noted that this solution converges to a constant $T = \beta(L - x) + T_0$ as $t \to \infty$. For $t > t_0$, to ensure the system of equations is well-posed for ablating solution to exist, the following constitutive relationship for β, β_m, T_0, T_m must be satisfied:

$$T_0 < T_m < \beta L + T_0, \quad \beta_m < \beta. \tag{60}$$

The first stage of the numerical simulation complies with the fixed boundary conditions, so the solution is comparable to the analytical solution (59). Then the model will automatically identify the instant t_0 when $T(0, t_0) = T_m$, and the simulation will be simultaneously switched to the second stage, i.e., the ablation mode in which an adaptive spatial grid conforming to the free boundary $s(t)$ is generated at each time step. Throughout the computation, uniform discretization in spatial and temporal directions is applied.

Hereafter, a case study is presented for the parameters set at $L = 1.0, \alpha = 1.0, \lambda = 0.6, \beta = 1.2, T_0 = -1, T_m = 0, \beta_m = 1, \Delta t = 0.001$. Table 2 presents the discrepancy between the analytical and numerical solution for temperature at the free boundary for $t < t_0$. As Table 1 shows, the two sets of results are in good agreement. In both cases the time when $T = T_m$ (ablation onset) is predicted at $t_0 = 0.64$. Figure 6 displays how the temperature and location of the free boundary evolve As Figure 6(a) shows, the temperature maintains constant at $T_m = 0$ after $t > t_0$. Different levels of refinement on the spatial grid indicate that the temperature for $t < t_0$ converges well with the analytical solution. Figure 6(b) presents the free boundary location $s(t)$ variation with time under the influence of ablation ($t > t_0$). Since the analytical solution is not available for this stage ($t > t_0$), a sensitivity study on the grid refinement was performed and found that $s(t)$ converges on the refinement level of $i_{max} = 1200 (\Delta x = 8.3e^{-4})$. Finally, an overview of the numerical solution in time and space is presented in Figure 7.

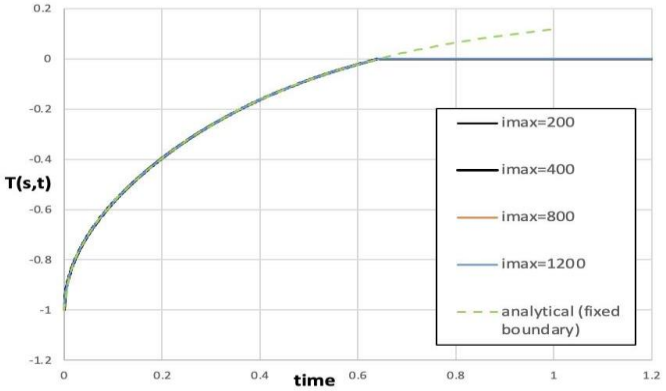

(a)

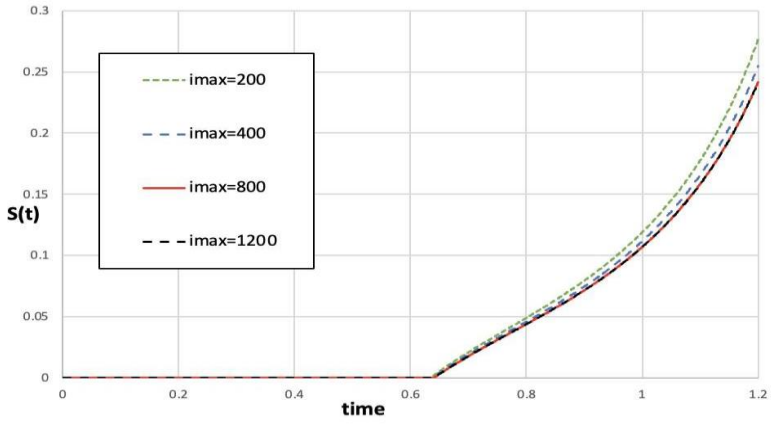

(b)

Figure 6. The evolution of the free boundary temperature *T*(*s*,*t*) and location s(t) before and after ablation over time: Δt = 0.001. (a) T(s,t) vs t; (b) s(t) vs t.

DOI: 10.54254/2753-8818/39/20240620

Table 2. Temperature vs time at the free boundary location prior to ablation: analytical vs numerical, $\Delta t = 1.e^{-3}, \Delta x = 8.3e^{-4}$

t	T_{ana}	T_{num}	diff. ratio
0.05	-0.697224	-0.69798	0.108%
0.1	-0.571812	-0.572348	0.094%
0.2	-0.395095	-0.395519	0.107%
0.3	-0.264117	-0.26455	0.164%
0.4	-0.162542	-0.162984	0.272%
0.5	-0.08326	-0.083691	0.518%
0.64	-0.000522	-0.000418	-19.9%(*)

Note (*): at t=0.64, the large ratio is due to the singularity. Physically the temperature at the boundary reaches the melting point of zero, i.e., the onset of ablation, in both the analytical and numerical solutions.

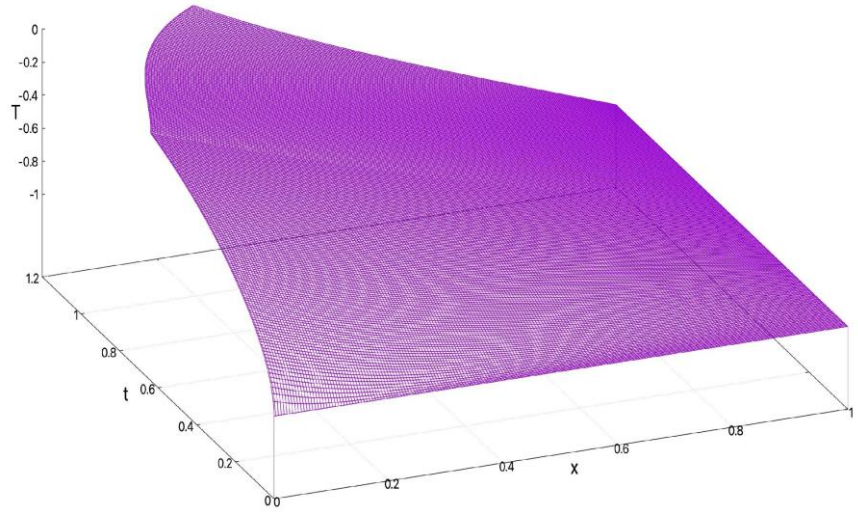

Figure 7. The overview of temperature and the free boundary location over time and space

4. Conclusions

This paper presents a numerical formulation that combines the finite-volume method with a time-dependent boundary-fitted coordinate system to tackle the moving boundary problems for the 1-D heat equation. Following the formulation process, an algorithm was created with the help of the linear algebra package Eigen to generate the data for the numerical solution. Four benchmark cases of heat conduction were investigated by this approach and compared to the analytical solution: a fixed boundary case, the liquid phase of a melting process, the solid phase of a melting process, and an ablating process. The results demonstrate the capability of the presented numerical formulation in efficiently solving the general 1 -D heat problems, especially the one-phase Stefan problems, as well as the consistency of the numerical and analytical solutions. Overall, the paper can be described as a study of Stefan problems and a demonstration of concepts for solving them. Thus, it's a type of work that advances a new idea and represents an advancement that could be built upon. Though this paper deals with only one dimension, the problem can be extended to higher dimensions for a better understanding of Stefan problems in real life. Stefan problems in general seek to describe phase changes in material, which constitutes a specific aspect of the heat equation. The work done in the paper demonstrates the solving of Stefan problems in such phase change scenarios, in the melting process (an ice cube melting) and liquid phase (a puddle of water). However, an additional ablation case involving the movement of the material in addition to the melting was also tested, which provides far-reaching implications. For example, the atmospheric re-entry of a spacecraft involves the ablation process due to the heating up of the moving vehicle. Although the paper does not specifically deal with these cases, further works can

DOI: 10.54254/2753-8818/39/20240620

build upon the demonstration of Stefan problems to develop an answer to certain problems. For example, as mentioned, Stefan problems can assist in creating a heat shield for atmospheric re-entry.

References

[1] Ewing M E Laker T S and Walker D T 2013 Numerical modeling of ablation heat transfer. Journal of Thermophysics and Heat Transfer 27 615–632.
[2] Javierre E Vuik C Vermolen F J and van der Zwaag S 2006 A comparison of numerical models for one-dimensional Stefan problems. Journal of Computational and Applied Mathematics, 192 445–459.
[3] Kar A and Mazumder J 1994 Analytic solution of the Stefan problem in finite mediums. Quarterly of Applied Mathematics 52 49–58.
[4] Kutluay S Bahadir A R and Ozdes A 1997 The numerical solution of one phase classical Stefan problem. Journal of Computational and Applied Mathematics 81 135–144.
[5] Mitchell S L and Vynnycky M 2009 Finite-difference methods with increased accuracy and correct initialization for one-dimensional Stefan problems. Applied Mathematics and Computation, 215 1609–1621.
[6] Mitchell S L and Vynnycky M 2012 An accurate finite-difference method for ablation-type Stefan problems. Journal of Computational and Applied Mathematics 236 4181–4192.
[7] Savovic S and Caldwell J 2009 Numerical solution of Stefan problem with time-dependent boundary conditions by variable space grid method. Thermal Science, 13 165–174.
[8] Stefan J 1891 Uber die theorie der eisbildung inbesondee uber die eisbindung im polarmeere. Ann. Phys U. Chem. 42 269–286.
[9] Tao L N 1981 Solidification of a binary mixture with arbitrary heat flux and initial conditions. Arch. Rat. Mech. Anal., 76 167–181.
[10] Thompson J F Soni B K and Weatherill N P 1999 Handbook of grid generation. CRC Press LLC.
[11] Greenberg M D 1998 Advanced engineering mathematics (Exercise 18.3, Prob. 17). Prentice Hall.